Available online at www.sciencedirect.com
SCIENCE DIRECT®
Minerals Engineering 18 (2005) 623–630
MINERALS ENGINEERING
This article is also available online at: www.elsevier.com/locate/mineng

Heap leaching kinetics are proportional to the irrigation rate divided by heap height

H.M. Lizama *, J.R. Harlamovs, D.J. McKay, Z. Dai

Teck Cominco Metals Ltd., Teck Cominco Research, P.O. Box 2000, Trail, BC, Canada V1R 4S4

Received 30 October 2004; accepted 16 December 2004

Abstract

Zinc sulphide ore was leached in columns of various heights and under various irrigation rates. Sphalerite and pyrite bioleaching kinetics agreed with the colonization shrinking core model where an initial colonization phase was followed by a steady rate phase. Columns irrigated at the same rate showed colonization rate constants (μ) of both sphalerite and pyrite that increased linearly with the inverse of column height. Similarly, the shrinking core rate constants (k) were also inversely proportional to heap height. When the irrigation rate was physically adjusted to compensate for height, columns ranging from 1 m to 8 m tall showed leaching curves that were identical. In essence, sphalerite and pyrite heap bioleaching kinetics were proportional to the irrigation rate divided by the height (L/h). The relationships governing the colonization and shrinking core rate constants were different for sphalerite and pyrite. Sphalerite bioleaching was favoured over pyrite at lower values of L/h. The degree of sulphur oxidation was favoured at higher values of L/h.

Keywords: Bioleaching; Heap leaching

1. Introduction

Heap bioleaching technology has been used for more than a decade in the copper and gold industries (Brierley and Brierley, 2001; Bhakta and Arthur, 2002), and recently has been piloted in the zinc industry (Lizama et al., 2003). The heaps are irrigated with leaching solution from the top, and are aerated with air forced in from the bottom. These heaps can range up to 10 m in height, and measure several hundred thousand m^2 in area. In general, heap leaching is simulated in columns charged with ore that are irrigated from the top and aerated from the bottom. Several column tests, and some small pilot heap tests, are required prior to design and construction of full-scale heaps. But even comprehensive column test programs do not guarantee accurate prediction of full-scale heap behavior. Clearly, robust and reliable parameters are needed to scale up bioleaching data from columns to heaps.

Recent experiments with short columns (1 m) revealed that bioleaching occurs in two stages. In the initial stage, bacteria come in contact with exposed sulphides and begin to multiply, colonizing the available sulphide mineral surface. In the second stage, only after the entire sulphide mineral surface is colonized and reacting, bioleaching follows shrinking core kinetics. This has been denoted the colonization shrinking core model (Lizama, 2004). In this model, the duration of the initial stage is determined by the colonization rate constant, μ (d^{-1}). Once the initial colonization stage is complete, the steady rate stage is determined by the shrinking core rate constant, k (d^{-1}). The values of these two constants determine the rate of sulphide mineral bioleaching. In this study, zinc sulphide ore was

* Corresponding author. Tel.: +1 250 364 4429; fax: +1 250 364 4400.
E-mail address: hector.lizama@teckcominco.com (H.M. Lizama).

0892-6875/$ - see front matter © 2005 Elsevier Ltd. All rights reserved.
doi:10.1016/j.mineng.2004.12.012

bioleached in columns of various heights and irrigated at various rates. The roles of these two variables on the constants μ and k were defined.

2. Materials and methods

2.1. Experimental procedure

Zinc sulphide ore was obtained from Teck Cominco's Red Dog Mine in Alaska, USA. The ore contained 15.0% zinc, 5.6% iron, 4.4% lead, and 13.0% sulphide sulphur. Lattice iron in sphalerite was 3%. This ore was crushed to −13 mm, resulting in a P_{80} size of 7.9 mm. The fines content (−150 μm fraction) was about 9.6%. Prior to loading into columns, this ore was agglomerated with water and sulphuric acid to a total moisture content of 8% and an acid addition of 10 kg/t.

The ore was bioleached in PVC columns (10 cm in diameter) at about 50 °C for 300–600 days. Depending on the height, each column contained between 32 kg and 263 kg of ore. The height of the columns ranged from 1 to 8 m. All columns were irrigated with raffinate solution from a zinc solvent extraction circuit (Lizama et al., 2003). This raffinate solution contained, on average, 12 g/L sulphuric acid, 12 g/L zinc, and less than 1 g/L iron. The raffinate solution E_h was about 640 mV SHE. Irrigation of the columns ranged from 0.03 L/m^2 min to 0.24 L/m^2 min. All the columns were aerated at a rate of 50 L/m^2 min. A water trap at the bottom of each column prevented incoming air from short-circuiting out with the pregnant leach solution (PLS) rather than traveling up the agglomerate bed. Each column was inoculated with a 50-mL mixed culture of the moderate thermophiles *Acidothiobacillus caldus* and *Sulfobacillus thermosulfidooxidans*. *A. caldus* is a strict sulphur oxidizer while *S. thermosulfidooxidans* oxidizes both ferrous ion and sulphur (Dopson and Lindström, 1999). This mixed culture had a density of about 10^8 cells/mL.

Solution throughputs to the columns were monitored by careful tabulation of PLS volumes. Raffinate solution and PLS were assayed every seven days for dissolved zinc and iron by atomic adsorption. The pH and E_h of raffinate and PLS were also measured. Free acid concentrations were determined by titration (Eaton et al., 1995). At the end of the tests, leached ore residues were weighed and assayed for moisture content. Final zinc, iron, lead, and total sulphur in residues were determined by incandescent plasma analyses.

2.2. Estimation of mass balances

In heap bioleaching, several chemical reactions occur simultaneously; individual metal extractions cannot be studied individually. The approach used was to examine all the bioleaching reactions simultaneously as described previously (Lizama, 2004):

$$ZnS + H_2SO_4 + 0.5O_2 \rightarrow ZnSO_4 + H_2O + S^o \quad (1)$$

$$FeS + H_2SO_4 + 0.5O_2 \rightarrow FeSO_4 + H_2O + S^o \quad (2)$$

$$FeS_2 + H_2SO_4 + 0.5O_2 \rightarrow FeSO_4 + H_2O + 2S^o \quad (3)$$

$$FeSO_4 + 0.5H_2SO_4 + 0.25O_2 \rightarrow 0.5Fe_2(SO_4)_3 + H_2O \quad (4)$$

$$S^o + 1.5O_2 + H_2O \rightarrow H_2SO_4 \quad (5)$$

$$PbS + 2O_2 \rightarrow PbSO_4 \quad (6)$$

Galena oxidation (Reaction (6)) had a very small effect on the ore material balance so it was ignored; less than 4% of the total sulphide sulphur was present as galena. Sphalerite oxidation (Reaction (1)) was measured from zinc leach data. Lattice iron oxidation (Reaction (2)) was calculated by multiplying the zinc leach data by the iron content in sphalerite. Pyrite bioleaching (Reaction (3)) was calculated by subtracting the calculated lattice iron value (Reaction (2)) from the overall iron leach data. Although pyrite does not oxidize according to Reaction (3) it is convenient for accounting purposes. Ferrous ion oxidation (Reaction (4)) was calculated from the iron content and measured E_h in PLS from the column. Overall sulphur oxidation (Reaction (5)) was calculated by subtracting the measured acid consumption from the sum of the stoichiometric acid demands for Reactions (1)–(4). Reactions (1)–(5) serve as a good approximation of bioleaching ore because they condense the various reactive chemical species into common measurable parameters.

2.3. Kinetic analyses of bioleach data

Sphalerite and pyrite bioleaching data were interpreted according to the colonization shrinking core model (Lizama, 2004). This model assumes that bioleaching occurs in two stages: ore is first activated as bacteria colonize the available mineral surface; but once colonization is complete the ore bioleaches following shrinking core kinetics. The pertinent equations used were

$$1 - 3(1-\alpha)^{2/3} + 2(1-\alpha) = k't \quad (7)$$

$$k' = \frac{k'_0 e^{(\mu t)}}{1 - \frac{k'_0}{k}[1 - e^{(\mu t)}]} \quad (8)$$

were α is the fraction of sphalerite or pyrite leached, t is time (d), k' is the observed rate constant (1/d), μ is the bacterial growth rate constant (1/d), k'_0 is the observed rate constant at the start of the reaction (1/d), and k is

the true value of the rate constant when bacterial colonization is complete and the reaction has reached a steady rate (1/d). The observed reaction rates, k' and k'_0, are related to k by

$$k' = \frac{C_{col}}{C_{MS}} k \tag{9}$$

$$k'_0 = \frac{C_{col,0}}{C_{MS}} k \tag{10}$$

where, C_{MS} is the concentration of sphalerite or pyrite surface available for bacterial colonization (cm^2/kg), C_{col} is the concentration of colonized sphalerite or pyrite surface (cm^2/kg), and $C_{col,0}$ is the concentration of colonized sphalerite or pyrite surface at the start of the test (cm^2/kg).

3. Results

3.1. Influence of column height and irrigation rate on bioleaching kinetics

Three columns of different heights were irrigated at the same rate: 0.17 L/m^2 min. These columns had agglomerate bed heights of 2 m, 6 m, and 8 m. Sphalerite and pyrite bioleaching data from these columns were plotted according to Eq. (7), as shown in Fig. 1. The three sphalerite data plots (Fig. 1A) became linear after activation periods of between 40 and 200 days. The activation periods for the pyrite plots were much longer (Fig. 1B). Linearity in these plots was not apparent until 200–500 days. The activation and steady rate stages of sphalerite and pyrite bioleaching are more apparent in Fig. 2, where plots of k' versus time are shown and are simply the derivatives of the curves in Fig. 1. The observed shrinking core rate constants, k', increased exponentially from k'_0 to k as bacteria colonized the sulphide mineral surface, with C_{col} increasing from $C_{col,0}$ to C_{MS}.

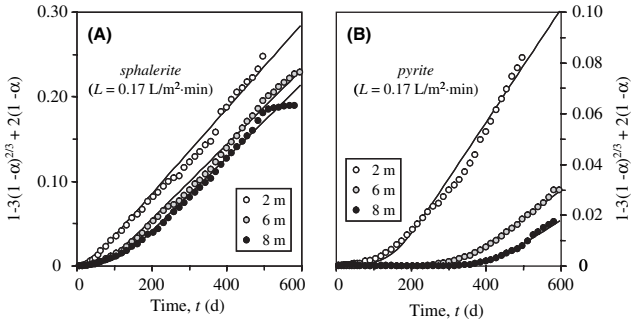

Fig. 1. Shrinking core plots of sphalerite leach data from columns of different heights (A); shrinking core plots of pyrite leach data from the same columns (B). All columns had the same irrigation rate. Model fit curves are included. Correlations of fit between data and model curves (R^2) were 0.99 or higher.

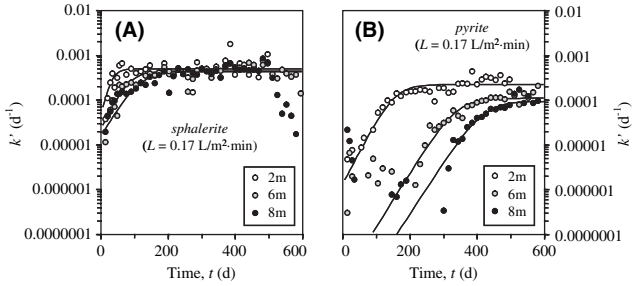

Fig. 2. Plot of the observed sphalerite rate constants, k', versus time for columns of different sizes (A); plot of the observed pyrite rate constants for the same columns (B). Data correspond to results obtained from Fig. 1. Model fit curves are included. Correlations of fit between data and model curves (R^2) ranged between 0.7 and 0.9.

The rate of exponential increases in k' were determined by the individual bacteria growth rate constants, μ. Model curves based on calculated values of k' are also included in the figure. The data sets in Fig. 2 behaved as predicted by Eq. (8). Figs. 1 and 2 show that colonization of sphalerite and pyrite by bacteria in tall columns was slower than in short columns. Even once colonization was complete, the rate of sphalerite and pyrite bioleaching was faster in short columns.

There was a lag between column start-up and onset of pyrite colonization in the tall columns; exponential increase in pyrite k was immediate only in the 2-m column (Fig. 2B). This was not so in the case of sphalerite, where the onset of colonization was immediate in all columns (Fig. 2A). This may have been due to the tall columns being acid limited during an initial period. Bioleaching reactions (1)–(4) consume acid; if the mass of ore being irrigated is very high in relation to the rate of acid delivery, the solution pH within the column will remain high for some time. This would cause precipitation of ferric ion that may affect pyrite leaching adversely. Initial acid limitation would have no such effect on sphalerite bioleaching. To account for the lag in observed pyrite colonization, artificially low k'_0 were inserted into the model equations.

Three columns, all having a 6-m-high agglomerate bed, were irrigated at different rates: 0.09 L/m^2 min, 0.17 L/m^2 min, and 0.36 L/m^2 min. Sphalerite and pyrite bioleaching data obtained from these columns were plotted according to Eq. (7), and are shown in Fig. 3. The sphalerite data plots in Fig. 3A all became linear after an activation period of about 100–200 days. As observed in past experiments, the activation periods for the pyrite plots were longer and showed more variability; the plots in Fig. 3B did not become linear until 150–450 days. Fig. 3 shows that the rate of sphalerite and pyrite bioleaching was faster with higher rates of irrigation. Initial periods of colonization by bacteria, however, did not did not appear shorter with higher irrigation rates. In summary, bioleaching of sphalerite

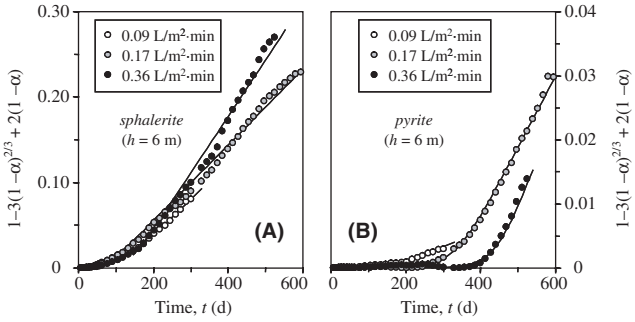

Fig. 3. Shrinking core plots of sphalerite leach data from columns irrigated at different rates (A); shrinking core plots of pyrite leach data from the same columns (B). All columns were 6-m tall. Model fit curves are included. Correlations of fit between data and model curves (R^2) were 0.9 or higher.

and pyrite was made faster by higher irrigation rates and shorter column heights.

3.2. Normalization of sphalerite and pyrite leaching

Given the results discussed in the previous section, a test was devised where the irrigation rate of a column was compensated for by its height. Four columns ranging in height from 1 to 8 m were irrigated at rates ranging from 0.03 to 0.26 L/m^2 min. In essence, all of these columns received identical volumes of solution per volume of agglomerate per unit of time, 0.03 L/m^3 min. The sphalerite and pyrite leach curves are shown in Fig. 4. As Fig. 4A shows, the sphalerite leach curves from the four columns were virtually identical. For sphalerite bioleaching, therefore, adjustment of the irrigation rates nullified the differences in column height. For pyrite bioleaching, Fig. 4B shows identical steady rates but the activation periods were different for the different column heights. The relationship between column height and irrigation rate was more complex for pyrite than for sphalerite.

Plots of k' versus time for sphalerite and pyrite are shown in Fig. 5. As expected, the sphalerite data plots can be superimposed (Fig. 5A). This means that the three sphalerite model parameters, k'_0, μ, and k, were identical when the irrigation rate was used to compensate for column height. In the case of pyrite, the three data plots had identical shapes but different intercepts (Fig. 5B). This means that the pyrite curves had identical values of μ and k but different values of k'_0. There was a lag between column start-up and onset of exponential increase in pyrite k' (see Fig. 5B). No such lag was observed with sphalerite; colonization was immediate (Fig. 5A). This lag in pyrite colonization was likely an acid limitation effect similar to that observed earlier (see Fig. 2B). The pyrite lag was observed in all columns, regardless of height; indicating that an L/h value of 0.03 L/m^3 min limited acid delivery to this ore. The pyrite k'_0 values at this L/h value were artificially low to account for the lag in colonization.

Ensuring that all the columns received identical volumes of solution per volume of agglomerate over time was accomplished by dividing the irrigation rate by column height and making sure this value was the same for all of the columns. The common values of k and μ evident in Fig. 5 indicate that these model parameters were related to irrigation rate and column height by the relationship:

$$k, \mu, k'_0 = f\left(\frac{L}{h}\right) \tag{11}$$

where L is the irrigation rate (L/m^2 min) and h is the column height (m). To confirm this relationship, k, μ, and k'_0 values from nine columns were plotted against their respective values of L/h. The nine columns varied in height and in irrigation rate but were all charged with the same agglomerated ore.

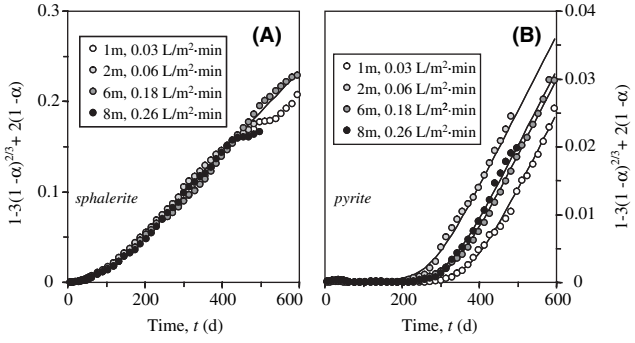

Fig. 4. Shrinking core plots of sphalerite leach data from columns where the irrigation rate was adjusted for height (A); shrinking core plots pyrite leach data from the same columns (B). All columns had the same irrigation to height ratio, L/h. Model fit curves are included. Correlations of fit between data and model curves (R^2) were 0.99 or higher.

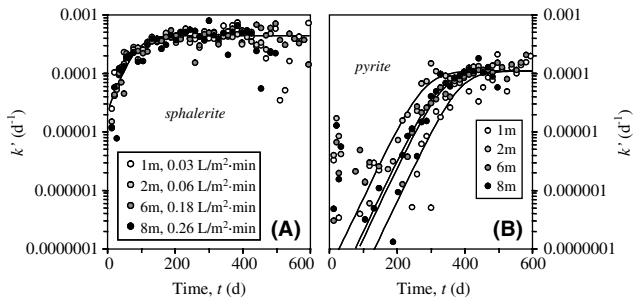

Fig. 5. Plot of the observed sphalerite rate constants, k', versus time for columns having the same irrigation to height ratio, L/h (A); plot of the observed pyrite rate constants for the same columns (B). Data correspond to results obtained from Fig. 4. Model fit curves are included. Correlations of fit between data and model curves (R^2) ranged between 0.71 and 0.95.

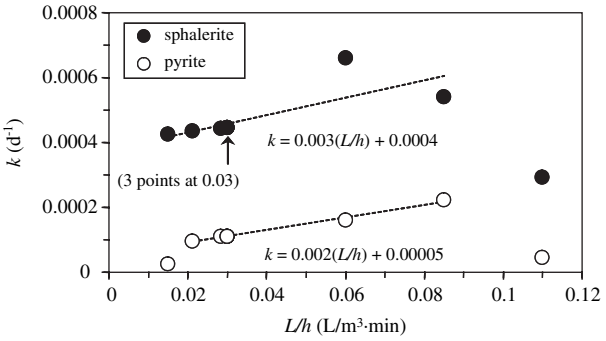

Fig. 6. Plot of k versus L/h for sphalerite and pyrite.

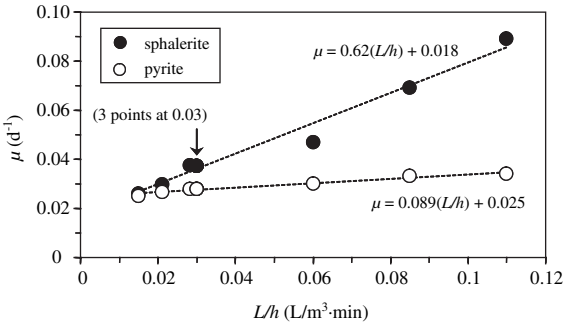

Fig. 7. Plot of μ versus L/h for sphalerite and pyrite.

Plots of the rate constant, k, versus L/h for sphalerite and pyrite from the nine columns are shown in Fig. 6. The figure includes values derived from the curves in Figs. 1 and 3. Over the range of L/h tested, k values for sphalerite were consistently much higher than those for pyrite, meaning that sphalerite bioleached much faster than pyrite. Sphalerite values of k increased linearly up to an L/h value of 0.085 L/m^3 min. If L/h increased beyond 0.085 L/m^3 min, the sphalerite k value decreased. Pyrite k values increased linearly only between L/h values of 0.02 L/m^3 min and 0.85 L/m^3 min. Above or below those L/h values, pyrite k values decreased sharply. The detrimental effect on sphalerite and pyrite k values by increasing L/h beyond 0.085 L/m^3 min was likely due to excessive irrigation of the agglomerated ore. Very high irrigation rates can destabilize the agglomerate particles, resulting in migration of fines, and compromising the ore bed's permeability to air and solution flow (Guzman et al., 1998). Typical irrigation rates used in copper heap leaching are in the order of 0.1 L/m^2 min (Brierley and Brierley, 2001; O'Brien et al., 2003; Bernal and Velarde, 2003). Given that these heaps are typically 6-m tall, the corresponding L/h value is only 0.02 L/m^3 min, one-fifth of the critical 0.085 L/m^3 min value observed in this study. The sharp decrease in k for pyrite but not for sphalerite at L/h below 0.02 L/m^3 min is likely an acidity effect. Since the bioleaching reactions consume acid (Reactions (1)–(4)), a rate of acid delivery that is too low will maintain a solution pH high enough to precipitate ferric ion, resulting in an underreporting of iron leaching. The column with the very low k value at L/h = 0.015 L/m^3 min showed a PLS pH that averaged 1.9 over its lifetime.

Plots of the bacterial growth rate constant, μ, versus L/h from all nine columns are shown in Fig. 7. Again, the figure includes values from Figs. 1 and 3. Both the sphalerite and pyrite colonization rate constants were directly proportional to L/h over the entire range tested. This means that even an excessive L/h did not interfere with the ore colonization process. Colonization of sphalerite was much faster than pyrite at higher L/h values. At very low L/h, however, colonization of the two minerals was very similar, as shown by the proximity of the respective μ values.

In contrast to the linear relationships with k and μ, plots of k'_0 versus L/h showed a power relationship, as shown in Fig. 8. The power curve for sphalerite k'_0 had a negative exponent value, meaning that higher L/h values hindered bacterial attachment to the mineral surface. According to Eq. (10), k'_0 depends on the initial concentration of mineral surface colonized, $C_{col,0}$, related to bacterial sorption to mineral surface (Lizama, 2004). Higher flows through the agglomerate bed mean shorter solution residence times, and less time for bacterial attachment. The pyrite k'_0 versus L/h power curve showed a positive exponent value, but this was an artifact due to delayed onset of pyrite colonization at low L/h values. The pyrite k'_0 values presented in Fig. 8 were adjusted downwards to account for the colonization lag. These lags were dominated by acid breakthrough in PLS; the time required for the PLS pH to drop below the 2.0 mark, where ferric ion precipitates. Fig. 9 illustrates how L/h, pH breakthrough, and pyrite colonization lag were all related. Increased L/h brought about a faster pH breakthrough in PLS (Fig. 9A), and the time to pH breakthrough corresponded, more or less, with the delay in onset of pyrite colonization (Fig. 9B).

3.3. Iron and sulphur oxidation

Proliferation of iron oxidizing bacteria in the columns was inferred from the change in PLS solution

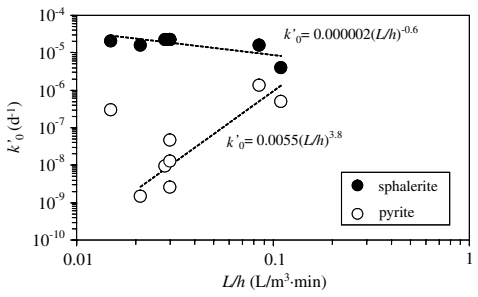

Fig. 8. Plot of k'_0 versus L/h for sphalerite and pyrite.

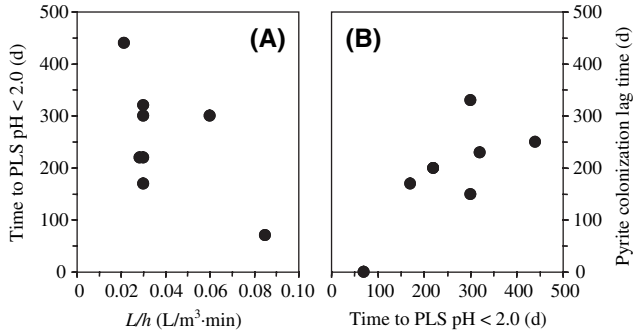

Fig. 9. Plot of PLS pH breakthrough time versus L/h (A); plot of pyrite colonization time lag versus pH breakthrough time (B). The pH breakthrough time is the time required for the PLS pH to drop below 2.0.

potential, E_h. This is because E_h is related to the ratio of dissolved ferric to ferrous ions, according to the Nernst equation (Rossi, 1990):

$$E_h = 771 + 59 \log \frac{C_{Fe3+}}{C_{Fe2+}} \quad (12)$$

where E_h is the solution potential (mV SHE), C_{Fe3+} is the ferric ion concentration (g/L), and C_{Fe2+} is the ferrous ion concentration (g/L). A bioleaching bacteria population growing exponentially on ferrous ion causes the ferric to ferrous ion ratio to increase; hence E_h is often used as an indicator of bioleaching activity. The PLS E_h from all columns in this study rose from about 500 mV to between 700 mV and 800 mV, within 200 days. Note that during this time pyrite leaching was insignificant; all soluble iron originated from bioleached sphalerite lattice iron (Reaction (2)). Fig. 10A shows the initial increases in E_h in three of the nine columns. The linear increases in E_h corresponded to net exponential increases in ferric ion concentration (Eq. (12)) and were analogous to growth curves of iron oxidizing bacteria. Since the bacteria-generated ferric ion was consumed in the partial oxidation of sphalerite (Reaction (1)), the slopes in Fig. 10A represented the differences between iron oxidation rates and sphalerite oxidation rates. As Fig. 10B shows, the E_h/t slopes increased logarithmically between L/h, values of 0.021 and 0.85 L/m^3 min. Above or below those L/h values, net ferric ion generation decreased drastically, as indicated by the very low E_h/t slopes (Fig. 10B). A very high L/h of 0.110 L/m^3 min had the same detrimental effect on net ferric generation as it did with the steady-rate constant for sphalerite and pyrite. The low E_h/t value at an L/h of 0.015 L/m^3 min can be explained by that column's acid limitation causing ferric precipitation.

Amounts of sulphide sulphur reacted and sulphur oxidized to sulphate were estimated using Reactions (1)–(5). This allowed the determination of sulphur oxidation in each column, as defined by

$$\text{sulphur oxidation} = \frac{\text{sulphide sulphur oxidized to sulphate}}{\text{sulphide sulphur reacted}} \times 100\% \quad (13)$$

Sulphur oxidation is an important parameter in heap leaching because it influences the overall acid balance of the process. Sulphur oxidation also influences the deportment of dissolved ferric ions by determining the pH breakthrough time in PLS; more sulphur oxidation generates more acid, lowers solution pH, and facilitates pH breakthrough. Fig. 11 compares PLS pH and sulphur oxidation at three different L/h values. As expected, increasing L/h, thereby increasing the rate of acid delivery, brought about faster pH breakthrough (Fig. 11A). But, surprisingly, faster L/h also resulted in more sulphur oxidation (Fig. 11B). About 60% of the reacted sulphide sulphur oxidized fully to sulphate over the course of the test when L/h was low (0.021 L/m^3 min). When L/h was high (0.085 L/m^3 min) sulphur oxidation increased from an initial 40% to almost 100%. The rate of acid delivery to a column is directly related to L/h; a column will be acid limited at a very low L/h. But acid limitation did not stimulate acid generation through sulphur oxidation. Instead, increasing the rate of acid delivery through increased L/h stimu-

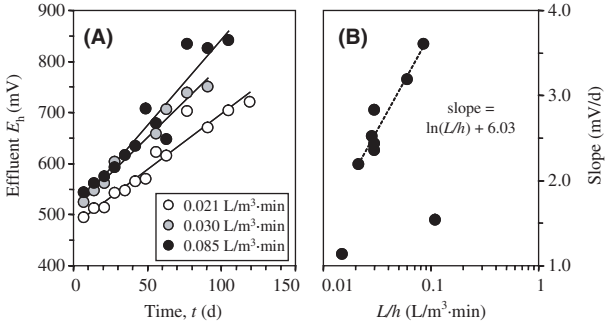

Fig. 10. Plot of PLS E_h versus time for three of nine columns (A); plot of E_h/time slopes from all nine columns versus L/h (B).

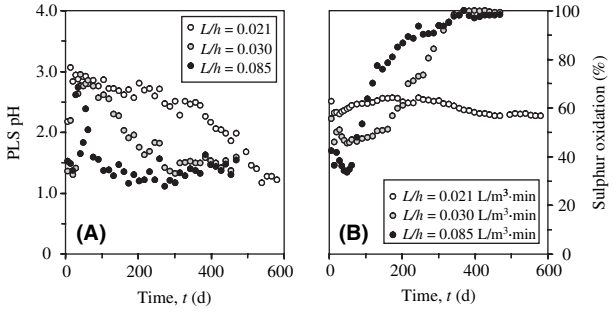

Fig. 11. Plot of PLS pH versus time for three columns with different L/h values (A); plot of sulphur oxidation versus time for the same three columns (B).

lated sulphur oxidation, generating more acid (Fig. 10B).

3.4. Modeling based on L/h

Column tests serve to simulate heap bioleaching. The results obtained with the various column tests allowed modeling of zinc heap leaching based on *L*/*h*. The *L*/*h* versus k, μ, and k'_0 relationships in Figs. 6–8 were used to predict the sphalerite and pyrite leach curves of hypothetical heaps stacked with ore similar to the one used in this study. The results are shown in Fig. 12. Only *L*/*h* values between 0.02 and 0.09 L/m^3 min were used, corresponding to the boundary conditions observed and described above. Below 0.02 L/m^3 min the theoretical heap would be acid limited, decreasing the pyrite leach rate significantly. Above 0.09 L/m^3 min the sphalerite and pyrite leach rates would also decrease significantly, probably due to localized flooding. From the sphalerite and pyrite leach curves in Fig. 12, instantaneous normalized leach rates were calculated and plotted in Fig. 13.

The leach curves in Fig. 12 show how bioleaching slows down at lower *L*/*h*. Decreasing *L*/*h* lengthens leach times required to achieve target recoveries. Furthermore, the *L*/*h*-based time requirements become longer as the target recovery is increased. The *L*/*h* effect on leach curves is stronger for pyrite than sphalerite; the sphalerite leach curves change relatively little compared to pyrite over the same range of *L*/*h*. This means that *L*/*h* has a strong effect on leaching selectivity between these two minerals. Lower *L*/*h* may decrease both minerals' bioleach rates but result in higher zinc to iron extraction ratios. The zinc to iron extraction ratio decreases with increasing *L*/*h*. The curves in Fig. 13 show how the instantaneous leach rates (%/d) peak and decline at different times according to *L*/*h*. The peak rate times are delayed as *L*/*h* decreases, again the effect being less pronounced for sphalerite than pyrite. This allows tailoring the leach time to maximize for the extraction of one mineral over another. For example, minimization of acid generation and iron extraction are key economic factors in zinc heap leaching because most of the acid and all dissolved ferric ion must be removed from PLS in order to not compromise the zinc solvent extraction circuit (Lizama et al., 2003).

Given the differential leaching effects and the effects on sulphur oxidation and ferric deportment, *L*/*h* shows potential as a design and operational tool for heap bioleaching. The various ways in which column leaching performance was influenced by *L*/*h* are summarized in Table 1. At high *L*/*h*, both sphalerite and pyrite bioleach rates are faster although the selectivity of the former is lower. A high *L*/*h* also results in more acid and ferric generation. At low *L*/*h*, bioleach rates of both sulphide minerals are slower but sphalerite selectivity is higher. There is also less acid and ferric generation at low *L*/*h*. The upper limit of *L*/*h* is dictated by the hydrodynamic properties of the agglomerate; at some point the high flow of solution will cause localized flooding and migration of fines. When the composition of the agglomerate

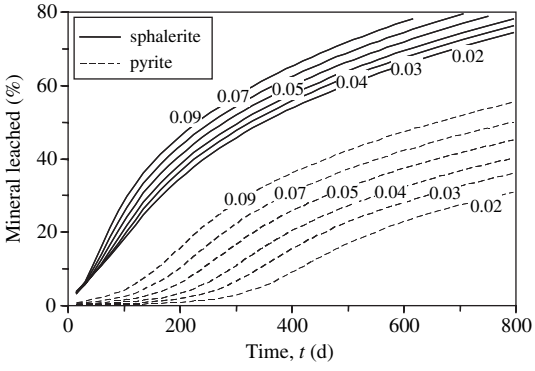

Fig. 12. Predicted leach curves of sphalerite and pyrite for hypothetical heaps operated at different *L*/*h* values.

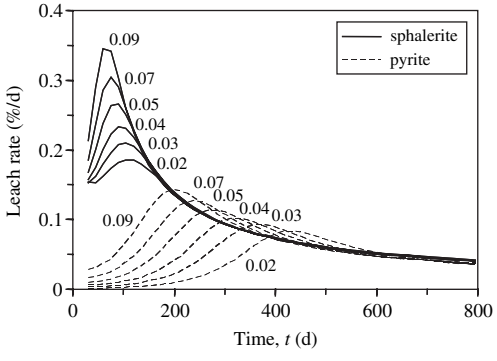

Fig. 13. Predicted instantaneous leach rates of sphalerite and pyrite for hypothetical heaps operated at different *L*/*h* values.

Table 1
Influence of *L*/*h* over bioleaching in columns or heaps

	Effect	Limiting conditions
Increase *L*/*h*	• Faster bioleach rate • Faster mineral colonization • Faster pH breakthrough • More sulphur oxidation/acid generation • Decreased selectivity in sphalerite vs pyrite bioleaching • Faster net ferric generation	• Flooding • Decomposition of agglomerate • Migration/ washout of fines
Decrease *L*/*h*	• Increased selectivity of sphalerite vs pyrite bioleaching • Less sulphur oxidation/acid generation • Slower net ferric generation • Slower pH breakthrough • Slower mineral colonization • Slower bioleach rate	• Acid limitation • Excessive ferric precipitation

is compromised, bioleaching rates will drop. The lower limit of L/h is determined by ore mineralogy: at a given flow rate the rate of acid delivery will be insufficient for the amount of sphalerite and pyrite under reaction. Ores with higher contents of sphalerite and pyrite will have higher acid requirements than lower grade ores.

4. Conclusions

The findings in this study identified the ratio of irrigation to height ratio, L/h, as a key parameter in heap bioleaching. This ratio controlled both the colonization and steady-rate stages of bioleaching, as well as the acid and iron balances. In addition, L/h served as a scale-up factor by normalizing leach curves from columns of different sizes (see Figs. 4 and 5). Adjusting solution flow to column height has been proposed as a scale-up factor in column testing of copper ores (Rood, 2000). In that study, leaching from columns of different heights was normalized by controlling the solution application volume, or L/h. That observation has now been made clear in the present study; the three kinetic parameters in bioleaching, k, k'_0, and μ are all functions of L/h. The relationships presented here serve not only for further understanding of heap leaching, but also for modeling purposes. Data from small column tests can be scaled up with good confidence to predict heap leach performance. Already existing heaps can be controlled by using L/h as an operational parameter.

Analyses and modeling of heap leach data using L/h does have its limitations. Conceptually, L/h is the normalized rate of reagent delivery to the ore. In this case, the reagent is a leach solution that contains acid, dissolved oxygen, and ferric ions. When two columns of different heights are irrigated at the same rate, the shorter column receives a greater amount of reagent per mass of reacting ore in a given time period. This faster reagent feed will result in a faster leach. But when two ores of different grades are leached in columns, they will have different reagent requirements and most likely will have different L/h relationships. Reagent delivery is already used as an operating parameter in copper heap leaching, where it is known as the irrigation ratio (Schlitt et al., 2003). The irrigation ratio is the total volume of leach solution applied to an ore bed, in m^3/t, to achieve a target copper recovery. Although this study quantified the effects of solution delivery, study of the delivery of those individual reagents (acid, ferric ion, dissolved oxygen) warrants further study.

Acknowledgment

The authors wish to thank Teck Cominco Metals Ltd. for permission to publish this work.

References

Bernal, O., Velarde, G., 2003. New technology for secondary sulfide heap leaching. In: Riveros, P.A., Dixon, D., Dreisinger, D.B., Menacho, J. (Eds.), Copper 2003–Cobre 2003, Hydrometallurgy of Copper, vol. VI. MetSoc, Montreal, pp. 177–188.

Bhakta, P., Arthur, B., 2002. Heap bio-oxidation and gold recovery at newmont mining: first-year results. JOM 54 (10), 31–34.

Brierley, J.A., Brierley, C.L., 2001. Present and future commercial applications in biohydrometallurgy. Hydrometallurgy 59, 233–239.

Dopson, M., Lindström, E.B., 1999. Potential role of *Thiobacillus caldus* in arsenopyrite bioleaching. Applied and Environmental Microbiology 65, 36–40.

Eaton, A.D., Clesceri, L.S., Greenberg, A.E., 1995. Standard Methods for the Examination of Water and Wastewater, 19th ed. American Public Health Association, Baltimore.

Guzman, A., Srivastava, R., Beale, G., 1998. A new method for estimating the hydraulic behavior of spent ore heaps, waste dumps, and tailing impoundments. In: Proceedings of the International Conference on Tailings and Mine Waste'98. 5th, Fort Collins, Colorado, January 26–28, Balkema, Rotterdam, pp. 263–271.

Lizama, H.M., 2004. A kinetic description of percolation bioleaching. Minerals Engineering 17, 23–32.

Lizama, H.M., Harlamovs, J.R., Bélanger, S., Brienne, S.H., 2003. The Teck Cominco HydroZinc™ process. In: Young, C.A., Alfantazi, A.M., Dreisinger, D.B., Harris, B., James, A. (Eds.), Hydrometallurgy 2003, vol. 2. TMS Publications, Warrendale, pp. 1503–1516.

O'Brien, M.F., Griffin, J.B., Cuthbertson, W.F., Lamanna, J.R., Wilton, L.E., 2003. Operational changes at Phelps Dodge's morenci mine. In: Riveros, P.A., Dixon, D., Dreisinger, D.B., Menacho, J. (Eds.), Copper 2003–Cobre 2003, Hydrometallurgy of Copper, vol. VI. MetSoc, Montreal, pp. 39–52.

Rood, E.A., 2000. Solution application techniques for column testing. Randol Copperx Hydromet Roundtable 2000. Randol International, Golden, pp. 49–52.

Rossi, G., 1990. Biohydrometallurgy. McGraw-Hill, Hamburg.

Schlitt, W.J., Hernández, R., López, M.E., 2003. The ROM leach testwork program at El Abra. ALTA 2003 Copper-8 Proceedings. ALTA Metallurgical Services, Castlemaine.